

# Robust Motion Control of the Frictionless Positioning Device Suspended by Cone-Shaped Active Magnetic Bearings

Ho-Seop Jeong

Samsung Electro-Mechanics, 314, Maetan 3 Dong, Paldal Ku, Suwon Si, Kyungki Do, Korea  
tel : 82-42-869-3056; fax : 82-42-869-3095; e-mail : hsjeong@sam.kaist.ac.kr

Chong-Won Lee

Center for Noise and Vibration Control(NOVIC), Department of Mechanical Engineering  
KAIST, Science Town, Taejon, Korea  
tel : 82-42-869-3016; fax : 82-42-869-8220; e-mail : cwlee@hanbit.kaist.ac.kr

*Abstract : A time delay controller with state feedback is proposed for the frictionless positioning device which is subject to the variations of inertia and the presence of measurement noise. The time delay controller, which is combined with a low-pass filter to attenuate the effect of measurement noise, ensures the asymptotic stability of the closed loop system. It is found that the low-pass filter tends to increase the robustness in the design of time delay controller as well as the gain and phase margins of the closed loop system. Simulation results support that the proposed controller guarantees a good tracking performance irrespective of the variation of inertia and the presence of measurement noise.*

## 1 Introduction

Active magnetic bearing(AMB) has nowadays been widely adopted in machines and robots, which are operated under the clean room and vacuum chamber environment. Particularly in semiconductor industry, the environment must be ultra-clean to prevent samples from contamination during handling and processing. In addition, magnetically suspended machines and robots have advantages such as active position control of the suspended part[1], control of force and stiffness of the handling point, and load sensing capability[2].

A frictionless positioning device suspended by cone-shaped AMBs is developed in the laboratory, which is driven by a brushless DC motor equipped with a resolver[3]. The device is capable of controlling three translational and two rotational motions by using four pairs of cone-shaped electromagnets, when the azimuth motion is controlled by a BLDC motor. Since such a system often has unknown, nonlinear, or time-varying parameters during operation, a good tracking performance is not likely to be achieved when we rely on a simple linear controller. In order to attain a desired performance for a system with some uncertainty, a linear controller normally requires re-tuning of the controller gains, otherwise a robust control law should be adopted.

Several robust control strategies have so far been proposed to control linear and nonlinear systems with uncertain dynamics or unknown parameters. Time delay control

(TDC) uses past observations regarding the system response and control input, in order to directly modify the control actions rather than adjusting controller gains or identifying system parameters [4]. Youcef-Toumi and Reddy[5] studied the TDC for high speed and high precision active magnetic bearings. In their work, experimental results indicated that the TDC has impressive static and dynamic stiffness characteristics for the prototype considered. Kelly[6] proposed a combination of the adaptive feed-forward control and the state feedback for position control of a DC servo motor, when variations in inertia or friction are present.

In this paper, a time delay controller with state feedback is proposed for the frictionless positioning device to achieve a desired tracking performance. In particular, the proposed control scheme is very effective for an inherently unstable system like AMB: the state feedback is to ensure the stability of the closed loop system and the incorporated time delay controller enables the exact tracking of the command input despite of the uncertainties. An outer loop is used to track the command input so that the system performance is not seriously affected. A simple first order low-pass filter is included to increase the robustness of TDC to the measurement noise. The stability of the controlled system in the discrete domain is analyzed using the Nyquist stability. Finally numerical simulations are performed to compare the tracking performance of the proposed controller against the conventional optimal controller.

## 2 Modeling of Frictionless Positioning Device

Figure 1 shows the schematic of the frictionless positioning device. Here,  $R_m$  and  $\beta$  are the effective radius and inclined angle of magnet core;  $b_1$  and  $b_2$  are the distances between two radial magnetic bearings from the C.G. point of the rotor;  $F_j, j=1$  to 8, is the magnetic force exerted by each magnet;  $(x, y, z)$  and  $(\theta_x, \theta_y, \theta_z)$  are the displacement and angular coordinates defined with respect to the mass center. The five d.o.f. linearized equations for the uncontrolled cone-shaped AMB system and the relation of voltage and current can be rewritten, with respect to the bearing fixed coordinate, as[3]

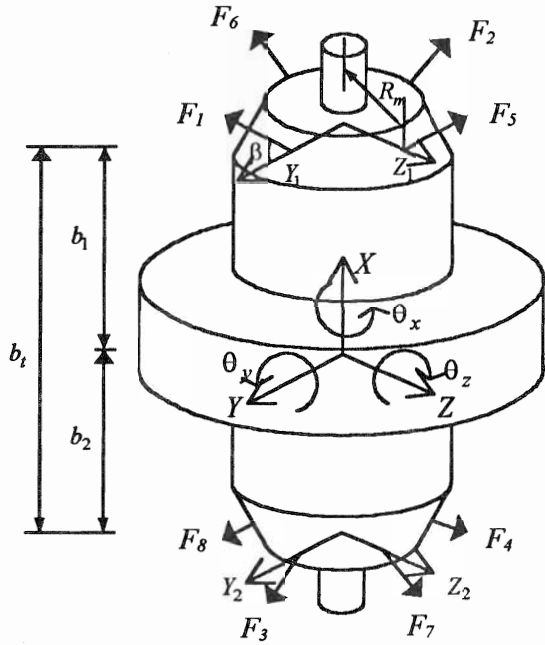


Fig. 1 Modeling of frictionless positioning device

$$\mathbf{M}_b \ddot{\mathbf{q}}_b + \mathbf{K}_b \mathbf{q}_b = \mathbf{K}_{ibm} \mathbf{i}_m \quad (1)$$

$$\tau_c \frac{d\mathbf{i}_m}{dt} = -\mathbf{i}_m + \mathbf{H}_c \mathbf{v}_c - \mathbf{D}_c \dot{\mathbf{q}}_b \quad (2)$$

where

$$\mathbf{q}_b = \{x, y_1, y_2, z_1, z_2\}^T,$$

$$\mathbf{i}_m = \{i_{y_1}, i_{y_2}, i_{y_3}, i_{y_4}, i_{z_1}, i_{z_2}, i_{z_3}, i_{z_4}\}^T,$$

$$\mathbf{v}_c = \{v_x, v_{y_1}, v_{y_2}, v_{z_1}, v_{z_2}\}^T$$

Here  $\mathbf{q}_b$  is the displacement vector defined in the bearing coordinate;  $\mathbf{i}_m$  is the control current vector;  $\mathbf{v}_c$  is the control voltage vector in the bearing coordinate;  $\mathbf{M}_b$ ,  $\mathbf{K}_b$  and  $\mathbf{K}_{ibm}$  are the mass, position stiffness and current stiffness matrices, respectively. For the conventional five d.o.f. AMB system controlled by five magnet pairs, only the diagonal terms are nonzero in the current and position stiffness matrices. On the other hand, for the cone-shaped AMB system, axial force also induces a moment because the magnetic forces exert perpendicular to the cone-shaped magnet face. The moment couples the upper and lower bearings, resulting in appearance of non-zero off-diagonal terms and decrease of negative diagonal terms in the position stiffness matrix. Note that the coupling effect increases as the ratio ( $r_m$ ) of the effective radius of magnet core,  $R_m$ , to the bearing span,  $b_b$ , and the inclined angle,  $\beta$ , increase.

In this designed system, the system is decoupled into five second order systems because the parameters  $r_m$  and  $\beta$  are small and the dynamics in the voltage to current relationships may be neglected when the corresponding pole ( $s = -1/\tau_c$ ) is located far left in the Laplace domain compared with the system poles[3]. Thus, from now on, we

will consider only the single-axis cone-shaped AMBs, and we can write the transfer function as

$$G_p(s) = \frac{K_{cq} K_{iq}}{m_q s^2 - K_q} = \frac{b}{s^2 - a^2} \quad (2)$$

or, in the state-space form, as,

$$\dot{\mathbf{x}}_p = \mathbf{A}_p \mathbf{x}_p + \mathbf{B}_p \mathbf{v}_q \quad (3)$$

$$\eta_p = \mathbf{C}_p \mathbf{x}_p$$

where

$$a = \sqrt{\frac{K_q}{m_q}}, \quad b = \frac{K_{cq} K_{iq}}{m_q}, \quad \mathbf{x}_p = \{q, \dot{q}\}^T,$$

$$q = x, y_1, y_2, z_1, z_2$$

$$\mathbf{A}_p = \begin{bmatrix} 0 & 1 \\ a^2 & 0 \end{bmatrix}, \quad \mathbf{B}_p = \begin{bmatrix} 0 \\ b \end{bmatrix}, \quad \mathbf{C}_p = [1 \quad 0]$$

Here  $q$  represents an element coordinate of  $\mathbf{q}_b$ ;  $m_q$  is the equivalent mass;  $K_q$  is the position stiffness;  $K_{iq}$  is the current stiffness;  $K_{cq}$  is the voltage-to-current gain;  $\mathbf{v}_q$  is the control input;  $b$  is the control input gain.

### 3 Controller Design

#### 3.1 Optimal Controller with Integral Action

When a state feedback controller is used to stabilize the inherently unstable AMB system, the steady-state position error may occur in case of tracking control. To eliminate the steady-state error, an integral action can be added to the existing state feedback controller as shown in Fig. 2. The integrator dynamics can be written as

$$\dot{z}_p = \eta_p \quad (4)$$

Introducing a new state vector,  $\mathbf{x} = \{z_p, \mathbf{x}_p\}^T$ , we can rewrite Eq.(3) as

$$\dot{\mathbf{x}} = \mathbf{A} \mathbf{x} + \mathbf{B} \mathbf{v}_q \quad (5)$$

$$\eta = \mathbf{C} \mathbf{x}$$

where

$$\mathbf{A} = \begin{bmatrix} 0 & \mathbf{C}_p \\ \mathbf{0} & \mathbf{A}_p \end{bmatrix}, \quad \mathbf{B} = \begin{bmatrix} 0 \\ \mathbf{B}_p \end{bmatrix}, \quad \mathbf{C} = \{0 \quad \mathbf{C}_p\}$$

Now consider the quadratic performance index given by[7]

$$J = \int_0^\infty (\mathbf{x}^T \mathbf{Q} \mathbf{x} + \mathbf{v}_q^T \mathbf{R} \mathbf{v}_q) dt \quad (6)$$

where  $\mathbf{Q}$  and  $\mathbf{R}$  are the positive semi-definite and positive weighting matrices, respectively. Then solution to the minimization of  $J$  is the optimal control law given by

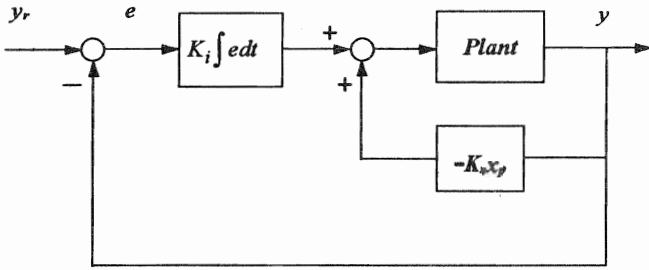


Fig. 2 Optimal controller with integral action

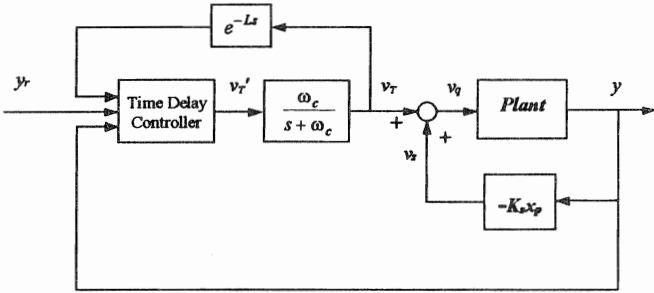


Fig. 3 Time delay controller with state feedback

$$v_q = -K_{opt} \mathbf{x} = -\begin{bmatrix} K_I & K_S \end{bmatrix} \begin{Bmatrix} z_p \\ \mathbf{x}_p \end{Bmatrix} \quad (7)$$

$$K_{opt} = \mathbf{R}^{-1} \mathbf{B}^T \mathbf{P}$$

where  $\mathbf{P}$  is the solution of the algebraic matrix Riccati equation.

When the system characteristics are known, designers can assign poles in the arbitrary locations by choosing the matrices  $\mathbf{Q}$  and  $\mathbf{R}$ . However, when the system has unknown, nonlinear or time varying characteristics, optimal controller with integral action may not guarantee a satisfactory performance. In that case, a time delay controller may be incorporated with the state feedback, as shown in Fig. 3. Use of an outer loop for the time delay controller enables exact tracking of step commands without seriously affecting system performance.

### 3.2 Time Delay Controller with State Feedback

A second order reference model is chosen as

$$\begin{aligned} \frac{dq_m}{dt} &= \dot{q}_m \\ \frac{d\dot{q}_m}{dt} &= -\omega_r^2 q_m - 2\zeta_r \omega_r \dot{q}_m + \omega_r^2 q_r \end{aligned} \quad (8)$$

where  $q_m(t)$  is the desired trajectory,  $q_r(t)$  is the reference input, and  $\omega_r$  and  $\zeta_r$  are the natural frequency and damping ratio of the second order reference model. The time delay control law is chosen to satisfy the requirement of Eq.(8) for single-axis cone-shaped AMB[4] of Eq. (3); i.e.

$$\begin{aligned} v_T(t) &= v_T(t-L) \\ &+ \frac{1}{\hat{b}} \left[ -\hat{q}(t-L) - \omega_r^2 q(t) - 2\zeta_r \omega_r \hat{q}(t) + \omega_r^2 q_r(t) \right] \end{aligned} \quad (9)$$

where  $\hat{q}$  and  $\hat{\dot{q}}$  are the estimates of the velocity and acceleration of the rotor,  $\hat{b}$  is the estimate of control input gain,  $b(q,t)$ , and  $L$  is the delay time. Note that the TDC law does not use any detailed information about the system. Instead, it requires accurate estimation of the velocity and acceleration from the measured displacement signal. On the other hand, signals are easily contaminated by measurement noises, which tend to be amplified in the velocity and acceleration estimation process. Low-pass filter is commonly used to smooth out such high frequency noises, but the filter dynamics should be taken into account in the controller design[8], as shown in Fig. 3. Knowing that the output from the controller is different from the input to the plant and letting the delay time  $L$  be equal to one sampling period in the digital implementation, we can modify the time delay controller of Eq.(9), in the discrete domain, as

$$\begin{aligned} v_T'(k) &= v_T(k-1) \\ &+ \frac{1}{\hat{b}} \left[ -\hat{q}(k-1) - \omega_r^2 q(k) - 2\zeta_r \omega_r \hat{q}(k) + \omega_r^2 q_r(k) \right] \end{aligned} \quad (10)$$

where  $v_T'(k)$  is the input to the filter and  $v_T(k)$  is the output from the filter. A first order low-pass filter can be approximated by a backward difference model, i.e.

$$v_T(k) = a_{f0} v_T(k-1) + a_{f1} v_T'(k) \quad (11)$$

where  $\omega'_c = \omega_c L$ ,  $a_{f0} = \frac{1}{1+\omega'_c}$ ,  $a_{f1} = \frac{\omega'_c}{1+\omega'_c}$ , and  $\omega_c$  is the cutoff frequency of the low-pass filter. As a result, the control input,  $v_q(k)$ , the sum of the state feedback outputs,  $v_s(k)$ , and time delay control output,  $v_T(k)$ , is written as

$$v_q(k) = v_T(k) + v_s(k) \quad (12)$$

where

$$v_s(k) = -K_s \mathbf{x}_p(k) = -K_p q(k) - K_d \hat{q}(k)$$

Here  $K_p$  and  $K_d$  are the proportional and derivative gains, respectively.

### 3.3 Stability Analysis

It will prove convenient to check the stability of the system by using the equivalent discrete system[9]. The plant dynamics can be approximated, by using the zero order hold method, as

$$G_p(z) = (1-z^{-1})Z\left[\frac{G_p(s)}{s}\right] = \frac{c(z+1)}{(z-e^{aL})(z-e^{-aL})} \quad (13)$$

where

$$c = \frac{b(e^{aL} - 1)^2}{2a^2 e^{aL}}$$

Referring to Fig. 3, we can rewrite the stabilized plant dynamics, by adding the state feedback, as

$$\frac{Q(z)}{U_T(z)} = \frac{c(z^2 + z)}{a_3 z^3 + a_2 z^2 + a_1 z + a_0} \quad (14)$$

where

$$a_0 = -\frac{cK_d}{L}, \quad a_1 = e^{aL} + cK_p,$$

$$a_2 = \frac{cK_d}{L} - e^{2aL} + cK_p - 1, \quad a_3 = e^{aL}$$

To estimate the velocity and acceleration from the measured displacement, we use the backward difference model given by

$$\hat{q}(k) \cong \frac{q(k) - q(k-1)}{L}, \quad \hat{\dot{q}}(k-1) \cong \frac{\hat{q}(k) - \hat{q}(k-1)}{L} \quad (15)$$

Then we can rewrite the discrete filtered time delay controller, using Eqs. (10) and (11), as

$$U_T(z) = -\frac{1}{\hat{b}(1/a_{f0}z - (a_{f0}/a_{f1} + 1))} \times \left\{ \left[ \omega_r^2 z + \frac{(z-1)^2}{zL^2} + 2\zeta_r \omega_r \frac{z-1}{L} \right] Q(z) - \omega_r^2 z Q_r(z) \right\} \quad (16)$$

Combining Eqs. (14) and (16), we can obtain the characteristic equation in the discrete domain as

$$1 + G(z) = 0 \quad (17)$$

where

$$G(z) = \frac{c(z^2 + z)}{\hat{b}(1/a_{f0}z - (a_{f0}/a_{f1} + 1))(a_3 z^3 + a_2 z^2 + a_1 z + a_0)} \times \left[ \omega_r^2 z + \frac{(z-1)^2}{zL^2} + 2\zeta_r \omega_r \frac{z-1}{L} \right]$$

Note that the system characteristics are determined by the sampling time,  $L$ , the estimation of control input gain,  $\hat{b}$ , and the cutoff frequency of first-order filter,  $\omega_c$ . The time delay controller essentially assumes for stability that the sampling time is very small. Figure 4 shows the Nyquist plot with the sampling time varied, for  $\omega_c = 500$  rad/sec,  $\omega_r = 5000$  rad/sec,  $\zeta_r = 1$ , and  $\hat{b} = 100$ . Note that the system becomes unstable as the sampling time exceeds a threshold

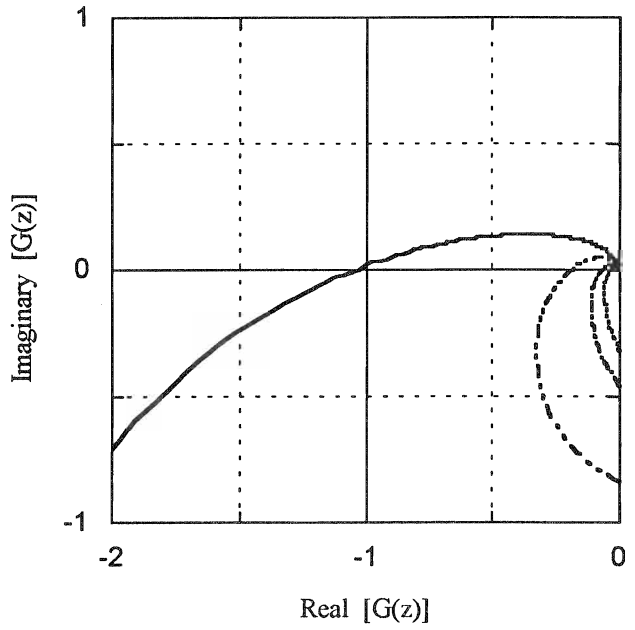


Fig. 4 Nyquist plot with sampling time varied:

—  $L=0.0009$ , - - -  $L=0.0005$ ,  
- · -  $L=0.0002$ , - - -  $L=0.0001$

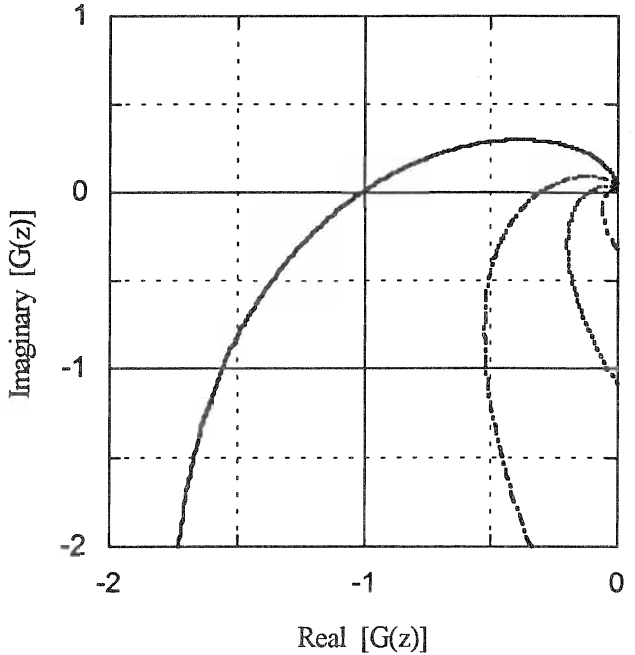


Fig. 5 Nyquist plot with  $b$  is varied:

— w/o filter, - - - w/ filter :  $b=30$   
- · - w/o filter, - - - w/ filter :  $b=100$

value  $L = 0.0009$  sec. The sampling time  $L = 0.0001$  sec. is a reasonable choice to guarantee the system stability. Figure 5 shows the Nyquist plot with  $\hat{b}$  varied, for  $\omega_c = 500$  rad/sec,  $\omega_r = 5000$  rad/sec,  $\zeta_r = 1$ , and  $L = 0.0001$  sec. Note that a low value of  $\hat{b}$  tends to destabilize the system, and that use of a low-pass filter increases the gain and phase margins.

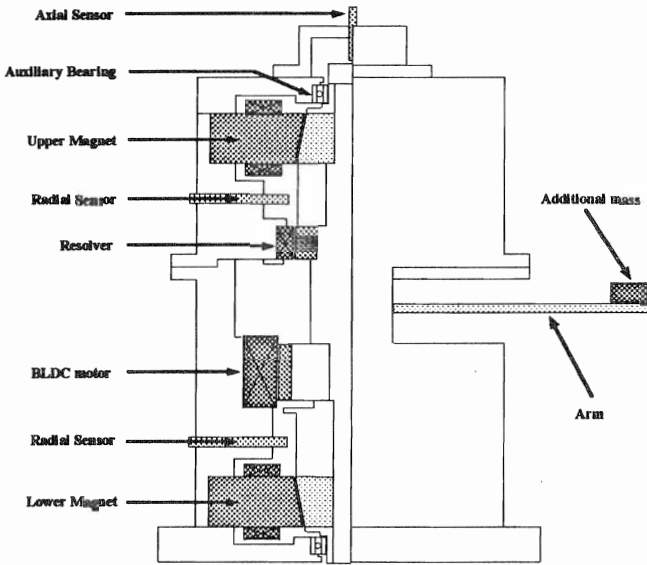


Fig. 6 Schematic of frictionless position device suspended by cone-shaped active magnetic bearings

4 Simulation

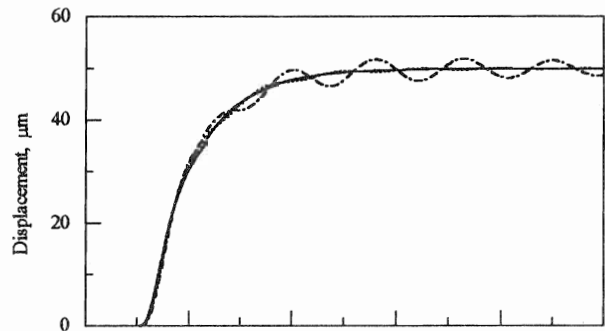
Figure 6 is the schematic of the tested frictionless positioning device. The system consists of a rotor, two radial cone-shaped AMBs, a driving BLDC motor, a resolver, and five eddy current type proximity probes. An additional mass is attached at the end of arm, as shown in Fig. 6. The system parameters are given in Table 1. In the simulations, we will show that the time delay controller with state feedback can indeed achieve a satisfactory tracking of a desired output trajectory. In addition, the effect of measurement noise on the system performance will be tested. The decentralized optimal and proposed controllers for the five d.o.f. system are designed using the methods described in section 3. Simulation results are presented for  $y_1$ -axis only, which is defined in Fig. 1, because of the similarity in the results for other axes. The parameter values throughout the simulations are given as:  $\omega_c = 500$  rad/sec,  $\omega_r = 5000$  rad/sec,  $\zeta_r = 1.0$ ,  $L = 0.0001$  sec., and  $\hat{b} = 100$ .

Figure 7 shows the step responses when the mass attached at the end of arm is varied. As shown in Fig. 7(a), optimal controller requires re-tuning of the controller gains to attain a desired tracking performance. On the other hand, the time delay controller with state feedback gives a good tracking performance even with the mass variation, as shown in Fig. 7(b).

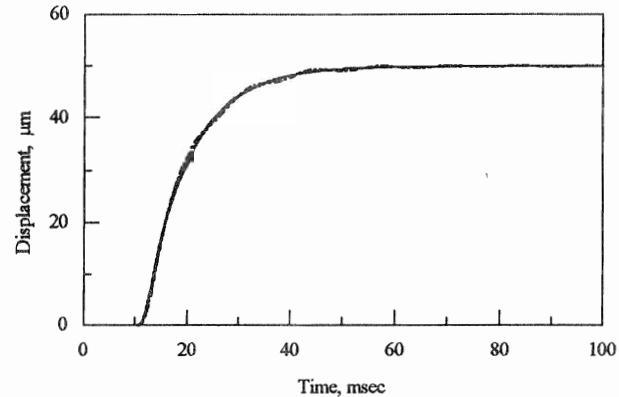
The effect of measurement noise on the system performance is important because time delay controller inherently includes the estimation of velocity and acceleration. In the simulations, a Gaussian white noise with the standard deviation  $\sigma=1.0 \times 10^{-11}$  is added to the displacement signals so that the noise is magnified by the backward difference algorithm in the estimation of velocity and acceleration. As shown in Fig. 8, we still get a stable system despite of the highly noisy estimations of velocity and acceleration. To deal with the undesirable high frequency noise in the

Table 1 Specifications of the designed frictionless positioning device

| Electro-Magnet and Rotor       |   |
|--------------------------------|---|
| Pole face area                 | $A = 18\text{mm} \times 10\text{mm}$                        |
| Air gap/ Rotor dia.            | $g_o = 0.5\text{mm} / \phi 43\text{mm}$                     |
| Inclined angle                 | $\beta = 10^\circ$  |
| Magnetic coils                 | $N=300, R=2\Omega, L_o=20\text{mH}$                         |
| Core lamination                | 0.1mm thick, 3% Si-steel                                    |
| Geometric factor               | $c=\alpha_g=0.92$   |
| Rotor mass                     | $m=1.86$ kg   |
| Polar moment of inertia        | $J_p=0.00121$ kg-m <sup>2</sup>                             |
| Dia. moment of inertia         | $J_d=0.00647$ kg-m <sup>2</sup>                             |
| Bearing span                   | $b_1=81.7\text{mm}, b_2=71.6\text{mm}$                      |
| Peripheral Electronic Devices  |   |
| Sensor & Amp.                  | Resolution : 0.5 $\mu\text{m}$<br>Gain $K_s=1\text{V/mm}$   |
| Linear Power Amp.              | Gain : $K_c=0.5$ A/V<br>Supply Voltage : $\pm 30\text{V}$   |
| BLDC Motor & Linear Power Amp. | Const. torque:0.28N-m<br>Angular excursion : $\pm 50^\circ$ |
| Resolver                       | Excite freq.:7Vrms,400Hz<br>Accuracy : $\pm 1'$             |



(a) optimal controller with integral action



(b) proposed controller

Fig. 7 Step responses with the attached mass varied: — Nominal; ..... 0.6K g; - - - - - 1.2K g

control input, an appropriate filter should be built for real-time applications. Figure 9 indicates that the proposed controller is slightly better in the noise rejection

performance than the optimal controller with integral action.

### 5 Conclusion

A time delay controller with state feedback is proposed for the frictionless position device and proven to be very effective throughout the simulations. The Nyquist stability analysis in discrete time domain shows that the proposed controller assures the system stability and that use of a low-pass filter tends to increase the gain and phase margins and to decrease the destabilization effect due to approximation in the discrete time domain. Simulation results support that the proposed controller guarantees a good tracking performance irrespective of the variations in inertia, the approximation effect, and the presence of measurement noise, compared with the conventional optimal controller.

### References

[1] A. Kuzin, M. Holmes, and D. Trumper, "Analysis and Design of the Control System for a Precision Magnetically-Suspended Six-Degree-of-Freedom Motion Control Stage," *Proceedings of MAG' 93 Magnetic Bearings, Magnetic Drives and Dry Gas Seals Conference*, Alexandria Virginia, pp65-73, 1993.

[2] T. Highchi, K. Oka, and H. Sugawara, "Development of Clean Room Robot with Contactless Joints using Magnetic Bearings," *Proceedings of USA-Japan Symposium on Flexible Automation*, Vol. 1, pp229-243, 1988.

[3] H. S. Jeong and C. W. Lee, "Dynamic Modeling and Optimal Control of Cone-Shaped Active Magnetic Bearing System," *Control Engineering Practice*, 1996.(submitted)

[4] K. Youcef-Toumi, O. Ito, "A Time Delay Controllers for Systems with Unknown Dynamics," *ASME Journal of Dynamic Systems, Measurement, and Control*, Vol. 112, pp133-142, 1990.

[5] K. Youcef-Toumi, S. Reddy, "Dynamic Analysis and Control of High Speed and High Precision Active Magnetic Bearings," *ASME Journal of Dynamic Systems, Measurement, and Control*, Vol. 114, pp623-633, 1992.

[6] R. Kelly, "A Linear-State Feedback Plus Adaptive Feed-Forward Control for DC Servomotors," *IEEE Trans. on Industrial Electronics*, Vol. 34, No. 2, pp153-157, 1987.

[7] B. D. O. Anderson, J. B. Moore, *Optimal Control - Linear Quadratic Methods*, Prentice-Hall, 1990.

[8] K. Youcef-Toumi, S. -T., Wu, "Input/Output Linearization Using Time Delay Control," *ASME Journal of Dynamic Systems, Measurement, and Control*, Vol. 114, pp10-19, 1992.

[9] K. Youcef-Toumi, J. Bobbett, "Stability of Uncertain Linear Systems with Time Delay," *ASME Journal of Dynamic Systems, Measurement, and Control*, Vol. 113, pp558-567, 1991.

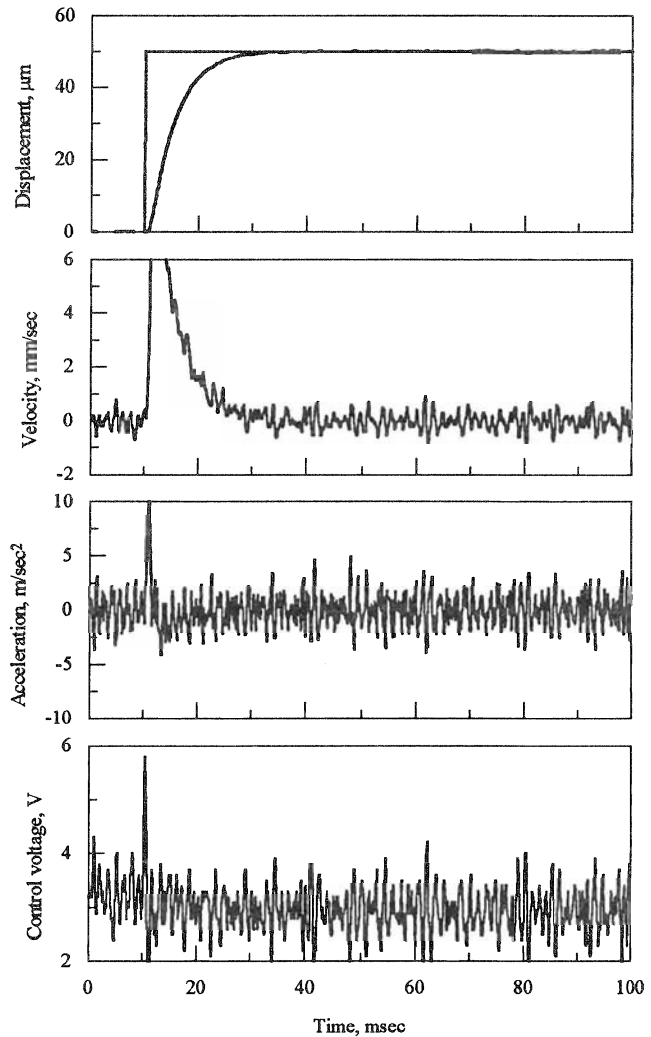


Fig. 8 Step response with noisy estimation ( $\sigma=1.0 \times 10^{-11}$ )

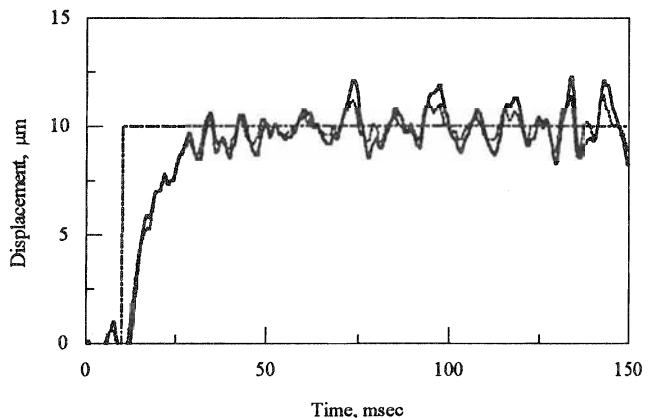


Fig. 9 Effect of the measurement noise:

— optimal controller; - - - - - proposed controller